RSC Advances

PAPER

View Article Online
View Journal | View Issue

Cite this: *RSC Adv.*, 2020, **10**, 8677

Detection of four phenolic oestrogens by a novel electrochemical immunosensor based on a hexestrol monoclonal antibody†

Guo-zheng Zhao,[a] Meng Wei,[b] Ya-juan Wang,[b] Xiu-wen Wang,[b] Hu Zhao,[c] Jian Shen*[b] and Bo Zhao*[b]

Received 1st January 2020
Accepted 17th February 2020

DOI: 10.1039/d0ra00006j

rsc.li/rsc-advances

Using a sandwich-type immunoassay, a novel electrochemical immunosensor based on the successful preparation of a hexestrol (HEX) monoclonal antibody was successfully constructed to detect four phenolic oestrogens: HEX, diethylstilboestrol (DES), dienestrol (DE) and bisphenol A (BPA). An innovative strategy to design the HEX monoclonal antibody/mercapto acetic acid (MACA)/nanogold immunosensor was developed by combining a nanosized effect, self-assembly and specific immune technology. The differential pulse voltammetry (DPV) response for four phenolic oestrogens was in the order BPA > DE > HEX > DES with detection limits of 0.037, 0.047, 0.052 and 0.060 ng mL^{-1}, respectively (S/N = 3). This immunosensor exhibits superior electrochemical properties with a wide linear range, low detection limit, excellent reproducibility and high selectivity. Compared with a high-performance liquid chromatography method, a high accuracy of DES detection in beef, duck and milk powder samples was achieved by the immunosensor proposed, which exhibits great potential for the detection of phenolic oestrogens in applications in environmental and food safety.

1. Introduction

Phenolic oestrogens are a group of organic compounds whose basic structure consists of a phenolic hydroxyl group or phenyl group,[1] which have been of wide and intense concern because they interfere with the processes of cell signalling,[2,3] resulting in information disorders *in vivo* when phenolic oestrogens enter the body.[4,5] They affect the expression of multiple genes during embryonic development,[6–8] resulting in metabolic dysfunction[9,10] and endocrine disorders as well as reproductive dysfunction of organisms.[11–13] Therefore, it is necessary to develop a rapid, sensitive and convenient method to detect the presence of phenolic oestrogens in the environment and foods.

Currently, the most commonly used methods for the detection of phenolic oestrogens in the environment and foods are high-performance liquid chromatography (HPLC),[14,15] gas chromatography-tandem mass spectrometry (GC-MS/MS),[16,17] liquid chromatography-tandem mass spectrometry (LC-MS/MS),[18–20] *etc.* In spite of its high accuracy, the common shortcomings of chromatography are that the analysis process is complex, multi-staged, and time-consuming, and there is a high cost for the instrumentation and reagents, and in addition they require professional technicians to operate the devices. It is difficult to achieve on-site detection with these methods and to meet the requirements of rapid and efficient detection.

An electrochemical immunosensor is a kind of detection instrument that uses an antigen–antibody specific immune response as a recognition element and displays the concentration changes of the target analyte through an electrochemical signal to achieve the purpose of detection.[21,22] As an analytical detection technology, it has developed rapidly in recent years and is suitable for the detection of bioactive molecules at very low concentrations, such as hormones, drugs, proteins and so on.[23] The significant improvement of nanotechnology provides the basis for the research of new materials and the introduction of application equipment with excellent performance. The unique chemical and electrical properties of nanomaterials make them widely used in many research fields, especially in the development of electrochemical sensor devices.[24] Furthermore, metal nanomaterials have been widely used in electrochemical immunosensors.[25] Currently, little research has been focused on the detection of phenolic oestrogens by electrochemical immunosensors.

In our recent work, Zhao *et al.* prepared an electrochemical immunosensor based on ractopamine (RAC)–bovine serum

[a]*Key Laboratory of Magnetic Molecules & Magnetic Information Materials, Ministry of Education, The School of Chemistry and Material Science, Shanxi Normal University, Linfen 041004, China*

[b]*National and Local Joint Engineering Research Center of Biomedical Functional Materials, Jiangsu Key Laboratory of Biofunctional Materials, School of Chemistry and Materials Science, Nanjing Normal University, Nanjing 210023, China. E-mail: jshen@njnu.edu.cn; zhaobo@njnu.edu.cn*

[c]*School of Life Science and Technology, China Pharmaceutical University, Nanjing 210009, China*

† Electronic supplementary information (ESI) available. See DOI: 10.1039/d0ra00006j

albumin antigens (BSAAs), suggesting attractive RAC detection with a broad linear range (1 to 1000 ng mL^{-1}) and low detection limit (0.25 ng mL^{-1}).[26] A electrochemical sensor with carboxymethyl-PEG-carboxymethyl (CM-PEG-CM) and a thrombin-binding aptamer (TBA) was reported to detect thrombin with a detection range of 1 pM to 160 nM and a detection limit of 1.56×10^{-14} M.[27] Furthermore, an electrochemical immunosensor that used adsorption of carcinoembryonic antibody (anti-CEA) on hyperbranched polyester nanoparticles with carboxylic acid functional groups (HBPE-CA)/Au NPs was developed, which presented an excellent signal response to carcinoembryonic antigen (CEA) with a detection range of 1–107 fg mL^{-1} and a detection limit of 0.251 fg mL^{-1}.[28] Therefore, electrochemical immunosensors can rapidly and conveniently detect their target analyte with high sensitivity in a broad linear range and have a low detection limit. Inspired by the merits of electrochemical immunosensors, after the successful preparation of a HEX monoclonal antibody, a novel HEX monoclonal antibody/MACA/nanogold electrochemical immunosensor was constructed in this work to detect four phenolic oestrogens (HEX, DES, DE and BPA) by a design strategy involving a nanosized effect, layer by layer self-assembly and antigen–antibody specific immune technology.

2. Experimental section

2.1 Reagents

HEX, DES, DE and BPA were purchased from Nanjing Wanqing Chemical Glassware Instrument Co., Ltd. Freund's complete and incomplete adjuvants, polyethylene glycol (PEG, M_w 1450), 1-cyano-4-dimethylaminopyridinium tetrafluoroborate (CDAP), horse radish peroxidase (HRP), hypoxanthine–thymidine (HT) Media Supplement (50×) Hybri-Max™, hypoxanthine–aminopterin–thymidine (HAT) Media Supplement (50×) HybriMax™, 3,3′,5,5′-tetramethylbenzidine (TMB) liquid substrate, mercapto acetic acid (MACA), acetonitrile, acetone, and *n*-hexane were supplied by Sigma-Aldrich. Dulbecco's modified Eagle medium (DMEM), foetal bovine serum (FBS) and bovine serum albumin (BSA, further purified fraction V, approx. 99%) were obtained from Gibco BRL, USA. HRP-conjugated polyclonal goat anti-mouse IgG and IgM antibodies were purchased from Boster Biological Technology Co., Ltd. *N*-Hydroxysuccinimide (NHS), carbodiimide hydrochloride (EDC), gold chloride tetrahydrate ($HAuCl_4 \cdot 4H_2O$), potassium ferricyanide, and potassium ferrocyanide were obtained from Sinopharm Chemical Reagent Co., Ltd. Phosphate buffer solution (PBS, 0.01 M, pH = 7.4) was prepared from potassium dihydrogen phosphate and sodium hydroxide. All other chemicals and reagents were of analytical grade. Redistilled water was used in all of the experiments. Beef, duck and the milk powder samples were purchased from a local supermarket.

2.2 Apparatus

Electrochemical measurements were performed by using a CHI600E electrochemical workstation (Shanghai Chenhua Apparatus Co., Ltd, China). A three-electrode system was used with platinum (Pt) wire, Ag/AgCl, and glassy carbon as the counter electrode, reference electrode, and working electrode, respectively. The morphologies of the modified electrodes were characterized using an S-4800 scanning electron microscope (SEM, Hitachi Instruments Co., Ltd, Japan). UV absorption spectra of the HEX, BSA and HEX–BSA complexes were measured by using a NanoDrop 2000 spectrophotometer (Thermo Fisher Scientific Inc., USA). The SDS-polyacrylamide gel electrophoresis (SDS-PAGE) of the HEX–BSA complex and proteins was performed using a Mini-Protean Tetra System (Bio-Rad Laboratories Inc., USA) and an Unstained Protein Molecular Weight Marker (Fermentas Inc. Canada) was used for molecular weight estimation.

2.3 Preparation of the HEX monoclonal antibody

2.3.1 Preparation of the HEX–BSA complex. First, 80 μL of CDAP (400 mM) in an acetonitrile solution was dropped into HEX (2 mL, 4.0 μM) in a HEPES buffer solution (0.15 M, pH 7.0), which was adjusted to pH 9.0 with 0.2 M triethylamine. Then, 80 μL of a BSA solution (66 mg BSA was dissolved in a 0.15 M HEPES buffer solution) was added to the above solution. The mixed solution was stored at 4 °C overnight and then we added 1 mL ethanolamine (1.0 M) in HEPES buffer solution (0.15 M), which was dialyzed (mwco, 8000–14 000 Da) with stirring against PBS (0.01 M, pH 7.4) for 24 h with two changes of fresh buffer to remove the uncoupled free hapten. Finally, the HEX–BSA complex was obtained and frozen at −20 °C before use.

2.3.2 Immunization. Several week-old BALB/c female mice were vaccinated intraperitoneally with 0.2 mL of an emulsion containing Freund's complete adjuvant and HEX–BSA complex (10 μg HEX–BSA complex per mouse). One similar booster vaccine was given a week later, but this complex was emulsified in Freund's incomplete adjuvant. Three days before cell fusion, the mice received the HEX–BSA alone (0.1 mg mL^{-1} in PBS with 0.2 mL per mouse) in the same manner.

2.3.3 Cell fusion, hybridoma selection and subcloning. Splenocytes from the immunized mice were fused with SP2/0 myeloma cells in the presence of PEG according to standard protocols. After HAT selection, the supernatants of the hybridoma cells were assayed by indirect ELISA (iELISA, described in the ESI†) for the presence of antibodies that recognized the complex. Then, the positive clones were transferred to 24-well plates. Five days later, these multiclones were screened again by indirect competitive ELISA (icELISA, described in the ESI†). Supernatants showing an inhibition of >80% in the presence of 10 mg mL^{-1} hapten compared to the absence of analyte were considered to be derived from high-affinity antibody-secreting hybridomas. Hybridomas with the desired characteristics were further subcloned and expanded for antibody production by being injected intraperitoneally into pristine primed BALB/c mice to obtain ascites fluid.

2.4 Construction of HEX monoclonal antibody/MACA/nanogold electrochemical immunosensor

A bare glassy carbon working electrode (GCE) was polished with 0.3 μm alumina powder and sonicated in ethanol/distilled water

(volume ratio 1 : 1) and distilled water consecutively for 40 s, then dried at room temperature for further use. Scheme 1 displays the preparation process of the HEX monoclonal antibody/MACA/nanogold electrochemical immunosensor based on the layer by layer self-assembly method. The treated GCE was immersed in 3 mM $HAuCl_4$ solution and electrodeposited at a constant voltage of −0.2 V for 60 s, then washed with distilled water and dried at room temperature. The modified electrode was immersed in MACA solution (1 mM, pH = 7.0) for 2 h at room temperature and self-assembled to form a MACA film. Furthermore, the modified electrode was saturated in 0.4 M EDC–0.1 M NHS solution to activate the carboxyl groups exposed on the surface of the electrode. Finally, 50 μL of HEX monoclonal antibody was coated on the electrode surface and placed at 4 °C overnight. To close the remaining active sites on the electrode surface, the modified electrode was saturated in 300 μL 0.5% BSA–PBS solution for 1 h to finish the HEX monoclonal antibody/MACA/nanogold electrochemical immunosensor, which was stored at 4 °C before use.

2.5 Pretreatment of real samples

2.5.1 Pretreatment of beef/duck sample. The beef/duck sample was crushed and weighed (1 g) into a 10 mL centrifuge tube. The standard solution of DES was added to the sample by the standard addition method to achieve a final DES concentration of 10, 50 and 200 ng mL^{-1} in three centrifugal tubes. Then, 3 mL acetonitrile–acetone extraction solution (volume ratio 4 : 1) was added. The mixture was sonicated and centrifuged for 30 and 10 min, respectively. The supernatant was transferred into centrifuge tube, dried under nitrogen at 50 °C, and mixed with 1 mL PBS (pH = 7.4). The extracts were dissolved and stored at 4 °C until detection.

2.5.2 Pretreatment of milk powder sample. The milk powder sample was weighed (0.3 g) into a 10 mL centrifuge tube. The standard solution of DES was added to the milk powder sample by a standard addition method to achieve a final DES concentration of 10, 50, or 200 ng mL^{-1}. Then, 2 mL of an *n*-hexane extraction solution was added. The mixture was sonicated and centrifuged for 30 and 10 min, respectively. The supernatant was transferred into test tubes, dried under nitrogen at 50 °C, and mixed with 1 mL PBS (pH = 7.4). The extracts were dissolved and stored at 4 °C until detection.

3. Results and discussion

3.1 Characterization of the HEX monoclonal antibody/MACA/nanogold immunosensor

The SEM images of the nanogold/GCE and the HEX monoclonal antibody/MACA/nanogold/GCE are shown in Fig. 1. Fig. 1A indicates that a large number of small bright spots with a uniform size (20–80 nm) are evenly distributed on the electrode surface. When the HEX monoclonal antibody is bound to the modified electrode surface, it can be seen that porous membranes appear in Fig. 1B. The HEX monoclonal antibody is embedded steadily and smoothly on the modified electrode surface due to the specific bonding interaction. This phenomenon illustrate that there is a stable combination between the HEX monoclonal antibody and the MACA modified on the surface of the electrode. In addition, it indirectly indicates that there is a stable bonding between the gold nanoparticles and MACA.

Fig. 1C describes the electrochemical impedance spectroscopy (EIS) of different kinds of electrodes with scanning frequency of 0.1 to 10^5 Hz, pulse amplitude of 5 mV s^{-1} in 5.0 mM $K_3[Fe(CN)_6]/K_4[Fe(CN)_6]$ (volume ratio 1 : 1). Under the set parameters, EIS shows good curves of different kinds of electrodes. The electron transfer resistance on the electrode surface (R_{ct}) is evaluated generally by its semicircular diameter

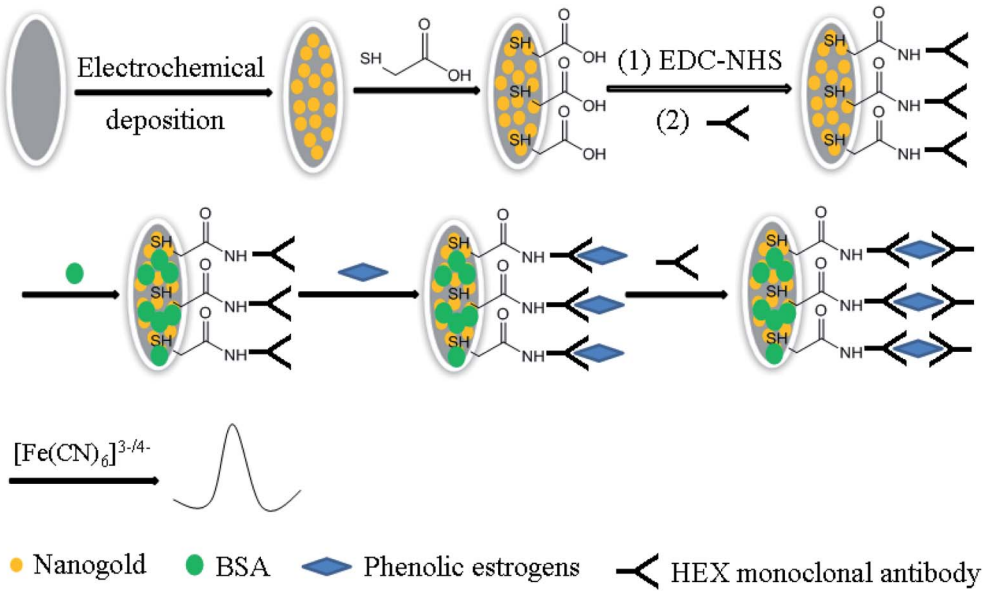

Scheme 1 Schematic depiction of the preparation process of the electrochemical immunosensor for detection of four phenolic oestrogens.

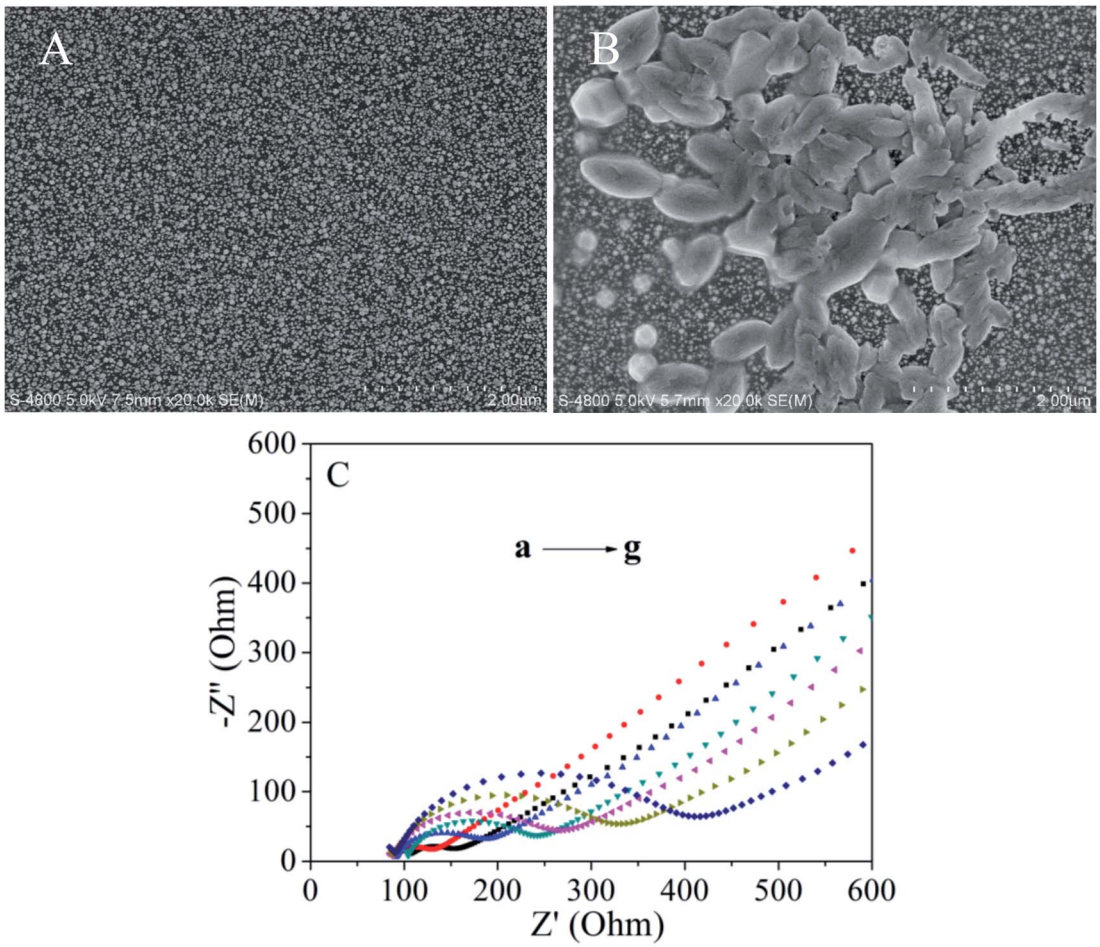

Fig. 1 SEM images of (A) nanogold/GCE and (B) HEX monoclonal antibody/MACA/nanogold/GCE. (C) EIS obtained in 0.1 mM KCl containing 5.0 mM $K_3[Fe(CN)_6]/K_4[Fe(CN)_6]$ (volume ratio 1 : 1) for (a) nanogold/GCE, (b) GCE, (c) MACA/nanogold/GCE, (d) HEX monoclonal antibody/MACA/nanogold/GCE, (e) BSA/HEX monoclonal antibody/MACA/nanogold/GCE, (f) DES/BSA/HEX monoclonal antibody/MACA/nanogold/GCE, (g) HEX monoclonal antibody/DES/BSA/HEX monoclonal antibody/MACA/nanogold/GCE.

in the high frequency zone. The larger the semicircular diameter, the more difficult the superficial electron transfer and the higher the charge transfer resistance R_{ct}. From Fig. 1C, the Nyquist diagram shows that the bare GCE exhibits a small semicircle at high frequencies, indicating that there is a low charge transfer resistance for bare GCE (curve b). When gold nanoparticles are modified on the GCE, the charge transfer resistance decreases significantly, meaning that nanoparticles

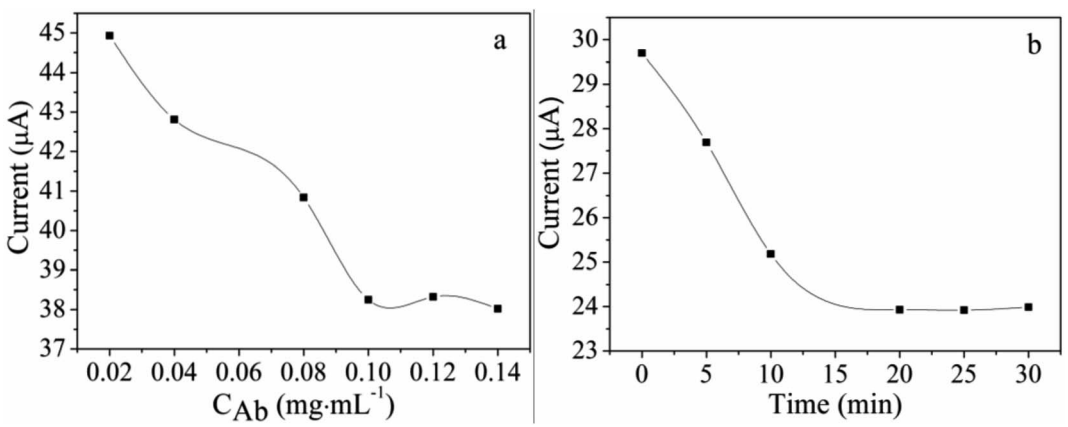

Fig. 2 Effect of (a) HEX monoclonal antibody concentration and (b) incubation time on the DPV peak current in the PBS solution (pH = 7.4) containing 2 mM $K_3[Fe(CN)_6]$.

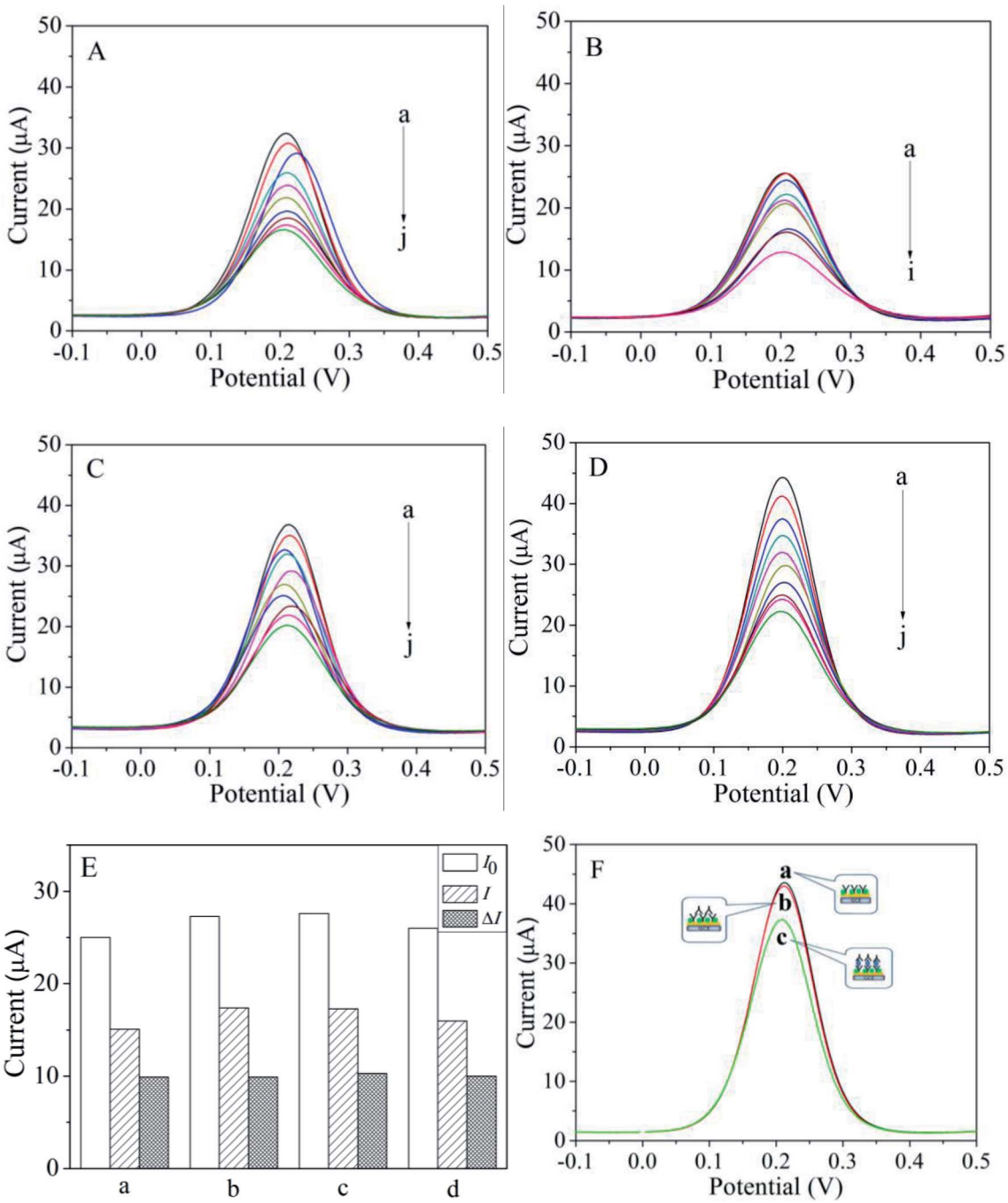

Fig. 3 DPV plots of different concentrations of standard solutions of (A) HEX, (B) DES, (C) DE and (D) BPA detected by the HEX monoclonal antibody/MACA/nanogold/GCE (a, b, c, d, e, f, g, h, i and j corresponding to concentrations from 0, 0.5, 1, 5, 10, 20, 50, 100, 200 and 500 ng mL^{-1}, respectively). (E) Selectivity of the HEX monoclonal antibody/MACA/nanogold/GCE was recorded by DPV with (a) 500 ng mL^{-1} methamidophos and 10 ng mL^{-1} DES, (b) 500 ng mL^{-1} dichlorvos and 10 ng mL^{-1} DES, (c) 500 ng mL^{-1} parathion and 10 ng mL^{-1} DES, and (d) 10 ng mL^{-1} DES. (F) DPV plots with variously modified electrodes in 2 mM $K_3[Fe(CN)_6]$ solution. (a) HEX monoclonal antibody/MACA/nanogold/GCE, (b) HEX monoclonal antibody and HEX monoclonal antibody/MACA/nanogold/GCE, (c) HEX monoclonal antibody, 10 ng mL^{-1} DES, and HEX monoclonal antibody/MACA/nanogold/GCE.

are a good conductive material and accelerate the electron transfer process (curve a). After modifying the MACA, fixing the HEX monoclonal antibody on the nanogold/GCE and blocking the nonspecific active sites by BSA, the value of the charge transfer resistance increases, which leads to an increase in the charge transfer barrier on the electrode surface (curves c, d and e). The prepared electrodes were incubated in 10 ng mL^{-1} DES solution for 90 min (curve f), then we added the HEX monoclonal antibody to form sandwich-type immune complexes (curve g). The charge transfer resistance increased typically, suggesting that the immune complexes further hinder charge transfer.

3.2 Optimization of conditions

Before detecting the phenolic oestrogens, the conditions involving the HEX monoclonal antibody concentration and incubation time were optimized as shown in Fig. 2. The electrodes' peak currents of differential pulse voltammetry (DPV) with different HEX monoclonal antibody concentrations and incubation times were evaluated in PBS solution (pH = 7.4) containing 2 mM $K_3[Fe(CN)_6]$. The scanning potential was −0.2 to 0.8 V and the scanning speed was 100 mV S^{-1}. The concentration of the HEX monoclonal antibody dropped on the MACA/nanogold/GCE plays an important role in the current value. The HEX monoclonal antibodies at different concentrations were coated on MACA/nanogold/GCE to investigate the impact on the current response at 37 °C. As shown in Fig. 2a, the current decreases with an increasing concentration of HEX monoclonal antibodies from 0.02 ng mL^{-1} to 0.10 ng mL^{-1}, then tends to be stable, implying the specific binding between the HEX monoclonal antibody and the MACA was saturated. Thus, the optimal concentration of HEX monoclonal antibody was identified as 0.10 ng mL^{-1}. The HEX monoclonal antibody/MACA/nanogold immunosensors were incubated in 200 ng mL^{-1} HEX solution for 90 min, then in 0.1 ng mL^{-1} HEX monoclonal antibody solution for 0, 5, 10, 15, 20, 25 or 30 min. As depicted in Fig. 2b, it is noticeable that the peak current of the immunosensor decreases gradually as the incubation time increases to 20 min due to the specific immune reaction between the HEX and HEX monoclonal antibody. After 20 min, the current value achieves a platform, illustrating the immune reaction was basically completed within 20 min. Therefore, 20 min was employed as the final incubation time.

3.3 Detection of four phenolic oestrogens

In this section, the electrochemical analysis of four phenolic oestrogens (HEX, DES, DE and BPA) with similar structures was carried out by using the constructed HEX monoclonal antibody/MACA/nanogold electrochemical immunosensor. The prepared HEX monoclonal antibody/MACA/nanogold electrochemical immunosensor was placed in a series of standard solutions of phenolic oestrogens with different concentrations. Specific adsorption occurred between phenolic oestrogens and HEX monoclonal antibodies modified on the surface of the electrode. Then it was incubated in the solution of HEX monoclonal antibody to form sandwich complex of antibody–antigen–antibody. Under the optimized experimental conditions, the performance of the HEX monoclonal antibody/MACA/nanogold/GCE was recorded by DPVs corresponding to different concentrations of phenolic oestrogens. As demonstrated in Fig. 3, the amperometric response decreased with increasing concentrations of HEX, DES, DE and BPA due to the specific immune reaction between the phenolic oestrogens and the HEX monoclonal antibody that inhibited electron transfer, which is consistent with the results from EIS analysis. At the same concentration, the amperometric response for BPA detection was stronger than those for the other detections in a sequence of BPA > DE > HEX > DES. In addition, the calibration graphs for HEX, DES, DE and BPA are presented in Fig. S2.†

The comparison (linear range, correlation coefficient and detection limit) of HEX, DES, DE and BPA detected by the HEX monoclonal antibody/MACA/nanogold/GCE is shown in Table 1. At the signal-to-noise ratio (S/N) of 3, the detection limits for HEX, DES, DE and BPA are 0.052, 0.060, 0.047 and 0.037 ng mL^{-1}, respectively, and the correlation coefficients are 0.9942, 0.9947, 0.9971 and 0.9931, respectively, proving that the HEX monoclonal antibody/MACA/nanogold immunosensor manifests outstanding performance with a wide linear range and low detection limit in comparison with previous methods used for phenolic oestrogens detection, for example, UFLC-MS/MS,[29] DLLME-CE,[30] micellar electrokinetic chromatography,[31] and capillary electrophoresis.[32] The wide linear range and low detection limit can be ascribed to the high specific area of the HEX monoclonal antibody/MACA/nanogold/GCE caused by the nanoscale effect and good conductivity of the gold nanoparticles, which increase the loading capacity of phenolic oestrogens and enhance electron transfer taking place at electrode surface. In addition, it ensures that the HEX monoclonal antibody can adhere to the electrode surface and be fixed in a larger amount, resulting in a stronger the specific immune reaction between phenolic oestrogens and HEX monoclonal antibody.

3.4 Reproducibility and selectivity

To measure the reproducibility of the HEX monoclonal antibody/MACA/nanogold/GCE, six concentrations of BPA were detected three times and the relative standard deviations of the HEX monoclonal antibody/MACA/nanogold immunosensor were 0.8%, 1.3%, 0.46%, 0.31%, 0.43% and 0.87%, corresponding to the BPA concentrations of 0.1, 0.5, 5, 20, 100 and

Table 1 Comparison of HEX, DES, DE and BPA detected by the HEX monoclonal antibody/MACA/nanogold/GCE

Phenolic oestrogens	Linear range (ng mL^{-1})	Correlation coefficient	Detection limit (ng mL^{-1})
HEX	0.5–1000	0.9942	0.052
DES	0.5–1000	0.9947	0.060
DE	0.5–500	0.9971	0.047
BPA	0.5–500	0.9931	0.037

Table 2 The reproducibility results of HEX monoclonal antibody/MACA/nanogold/GCE

BPA (ng mL^{-1})	Current (μA)	BPA (ng mL^{-1})	Current (μA)
0.1	43.60	20	29.78
	44.87		30.12
	42.78		29.58
0.5	41.14	100	24.99
	40.90		25.17
	41.20		24.55
5	34.69	500	22.15
	34.01		21.91
	34.92		23.02

Table 3 Test results of real samples after adding the DES standard solution

Real samples	Amount added (ng mL^{-1})	Amount measured (ng mL^{-1})	Recovery (%)	RSD (%)
Beef	10	9.11 ± 0.60	91.13	6.60
	50	47.64 ± 2.13	95.28	4.46
	200	221.98 ± 11.38	110.99	5.12
Duck	10	10.25 ± 1.32	102.47	12.92
	50	47.22 ± 5.51	94.44	11.66
	200	206.73 ± 9.22	103.37	4.46
Milk powder	10	10.1 ± 0.53	101.04	5.24
	50	54.37 ± 5.04	108.72	9.27
	200	181.45 ± 11.37	90.72	6.27

500 ng mL^{-1}, respectively, demonstrating the prepared immunosensor has satisfactory reproducibility (Table 2). The selectivity of the HEX monoclonal antibody/MACA/nanogold/GCE was investigated according to the DPV response, which is displayed in Fig. 3E. Several interfering components (methamidophos, dichlorvos and parathion) were selected and added to the DES solution to test the selectivity of the prepared immunosensor. In a 10 ng mL^{-1} DES solution, 500 ng mL^{-1} methamidophos (a), 500 ng mL^{-1} dichlorvos (b) and 500 ng mL^{-1} parathion (c) were added, respectively, then incubated in HEX monoclonal antibody solution. The initial DPV current value I_0 and current value I of the modified electrode after incubation were recorded. As shown in Fig. 3E, there was no significant difference between the current changes ΔI after incubation in the solutions containing interference components and that in the solution containing 10 ng mL^{-1} DES (d), implying that the proposed immunosensor has excellent selectivity for DES detection, which can be attributed to the specific recognition between the HEX monoclonal antibody and DES. Whether non-specific interactions of HEX monoclonal antibodies occur was also investigated based on the DPV response, which is shown in Fig. 3F. HEX monoclonal antibody was added to the HEX monoclonal antibody/MACA/nanogold/GCE directly without any detectable substance present, and the signal response was assessed by DPV. As shown in Fig. 3F, curve a shows the DPV response of the HEX monoclonal antibody/MACA/nanogold/GCE. Curve b is basically the same as curve a, from which it can be concluded that the non-specific adsorption between HEX monoclonal antibodies is not obvious in the absence of detectable substances. After adding 10 ng mL^{-1} DES, the current peak of curve c decreased. The reason for this is that the HEX monoclonal antibody is highly specific for the recognition of phenolic oestrogens, and the non-specific adsorption is effectively blocked in the preparation of the immunosensor. The electrochemical signal response comes from the specific antigen–antibody reaction, which indicates that the immunosensor has attractive anti-interference abilities.

3.5 Analysis of real samples

To examine the practical applicability of the immunosensor, the investigation of DES in real beef, duck and milk powder samples was also performed. Different DES concentrations were added to the real samples by a standard addition method. Table 3 describes three different DES concentrations in real samples detected by the constructed immunosensor. The average recoveries from beef, duck and milk powder are 91.13–110.99%, 94.44–103.37% and 90.72–108.72%, respectively. To verify the accuracy of the immunosensor, beef samples were detected by high-performance liquid chromatography without the addition of the DES standard solution. The results showed that there is no DES in the beef samples. Therefore, the constructed immunosensor has high accuracy and can be effectively used for real sample detection.

4. Conclusions

In this case, a HEX monoclonal antibody was prepared successfully by constructing a combination of HEX and BSA, immunization, cell fusion, hybridoma selection and subcloning; the antibody was then favourably used to fabricate the HEX monoclonal antibody/MACA/nanogold electrochemical immunosensor to achieve the detection of four phenolic oestrogens (HEX, DES, DE and BPA). Compared with previous detection methods, the HEX monoclonal antibody/MACA/nanogold/GCE displays a noticeably good performance, which is attributed to the specific immune reaction between phenolic oestrogens and the HEX monoclonal antibody. The signal response for the detection of four phenolic oestrogens is in the sequence of BPA > DE > HEX > DES with the same order corresponding to a detection limit of 0.037, 0.047, 0.052 and 0.060 ng mL^{-1}, respectively (S/N = 3). This multi-residue electrochemical immunosensor based on a HEX monoclonal antibody has a wide linear range, low detection limit, and high reproducibility and selectivity. In addition, the nanosized effect and specific antigen–antibody reaction possess an irreplaceable effect in the constructed novel immunosensor, producing wonderful electrochemical properties. Furthermore, the novel design strategy combining nanosized effect, self-assembly and specific immune technology will provide a feasible approach to construct excellent immunosensors that can then be applied to environmental and food safety detection.

Live subject statement

All experiments were performed in compliance with the Guidelines for Care and Use of Laboratory Animals of China Pharmaceutical University and were approved by the Animal Ethics Committee of Jiangsu Laboratory Animal Center.

Conflicts of interest

There are no conflicts to declare.

Acknowledgements

This work was supported by Linfen Key Research and Development Projects (Social Development) (No. 1909), Cultivation Plan of Young Scientific Researchers in Higher Education Institutions of Shanxi Province, Scientific and Technologial Innovation Programs of Higher Education Institutions in Shanxi (No. 2019L0469), Technology Support Program of Science and Technology Department of Jiangsu Province (BE2015703), Huaian Key Research and Development Program (HAS201619) and the Fund for Shanxi "1331 Project".

References

1 K. Petersen, M. T. Hultman, S. J. Rowland and K. E. Tollefsen, *Aquat. Toxicol.*, 2017, **190**, 150.
2 Z. L. Xin, X. Wu, T. Ji, B. P. Xu, Y. H. Han, M. Sun, S. Jiang, T. Li, W. Hu, C. Deng and Y. Yang, *Pharmacol. Res.*, 2019, **141**, 208.
3 A. Siddique, H. Y. Ebrahim, M. R. Akl, N. M. Ayoub, A. A. Goda, M. M. Mohyeldin, S. K. Nagumalli, W. M. Hananeh, Y. Y. Liu, S. A. Meyer and K. A. El Sayed, *Nutrients*, 2019, **11**, 412.
4 T. Baluchnejadmojarad, N. Rabiee, S. Zabihnejad and M. Roghani, *Brain Res.*, 2017, **1662**, 23.
5 C. Spagnuolo, G. L. Russo, I. E. Orhan, S. Habtemariam, M. Daglia, A. Sureda, S. F. Nabavi, K. P. Devi, M. R. Loizzo, R. Tundis and S. M. Nabavi, *Adv. Nutr.*, 2015, **6**, 408.
6 W. H. Qiu, H. Y. Shao, P. H. Lei, C. M. Zheng, C. X. Qiu, M. Yang and Y. Zheng, *Chemosphere*, 2018, **194**, 1.
7 D. Crump, S. Chiu and K. L. Williams, *Environ. Toxicol. Chem.*, 2018, **37**, 530.
8 Y. J. Jeong, C. H. An, S. C. Park, J. W. Pyun, J. Lee, S. W. Kim, H. S. Kim, H. R. Kim, J. C. Jeong and C. Y. Kim, *J. Agric. Food Chem.*, 2018, **66**, 4099.
9 F. V. Hassani, K. Abnous, S. Mehri, A. Jafarian, R. Birner-Gruenberger, R. Y. Robati and H. Hosseinzadeh, *Food Chem. Toxicol.*, 2018, **112**, 26.
10 V. Padmanabhan and A. Veiga-Lopez, *J. Anim. Sci.*, 2014, **92**, 3199.
11 R. G. Ahmed, *Food Chem. Toxicol.*, 2016, **95**, 168.
12 R. Rezg, S. El-Fazaa, N. Gharbi and B. Mornagui, *Environ. Int.*, 2014, **64**, 83.
13 Y. Peng, K. H. Nicastro, T. H. Epps and C. Q. Wu, *J. Agric. Food Chem.*, 2018, **66**, 11775.
14 B. B. Chen, Y. L. Huang, M. He and B. Hu, *J. Chromatogr. A*, 2013, **1305**, 17.
15 J. Wang, C. S. Cheng and Y. L. Yang, *J. Food Sci.*, 2015, **80**, 2655.
16 B. Albero, C. Sanchez-Brunete, E. Miguel and J. L. Tadeo, *Anal. Methods*, 2015, **7**, 3006.
17 C. L. Ke, Z. H. Wang, J. L. Gan, Y. G. Gu, K. Huang, L. D. Li and Q. Lin, *RSC Adv.*, 2014, **4**, 2355.
18 H. Chang, X. Y. Shen, B. Shao and F. C. Wu, *Environ. Pollut.*, 2018, **235**, 881.
19 M. Celic, S. Insa, B. Skrbic and M. Petrovic, *Anal. Bioanal. Chem.*, 2017, **409**, 5427.
20 Y. H. Qin, J. R. Zhang, Y. J. Li, Y. T. Han, N. Zou, Y. B. Jiang, J. H. Shan and C. P. Pan, *Anal. Bioanal. Chem.*, 2016, **408**, 5801.
21 P. Supraja, S. Tripathy, S. R. K. Vanjari, V. Singh and S. G. Singh, *Sens. Actuators, B*, 2019, **285**, 317.
22 J. Qi, B. W. Li, N. Zhou, X. Y. Wang, D. M. Deng, L. Q. Luo and L. X. Chen, *Biosens. Bioelectron.*, 2019, **142**, 111533.
23 X. G. Sun, B. W. Li, C. Y. Tian, F. B. Yu, N. Zhou, Y. H. Zhan and L. X. Chen, *Anal. Chim. Acta*, 2018, **1007**, 33.
24 X. M. Zhuang, D. D. Chen, S. N. Wang, H. T. Liu and L. X. Chen, *Sens. Actuators, B*, 2017, **251**, 185.
25 G. P. Pan, G. Z. Zhao, M. Wei, Y. J. Wang and B. Zhao, *Chem. Phys. Lett.*, 2019, **732**, 136657.
26 M. Shi, Y. Yan, Y. J. Hu, S. L. Liu, C. Y. Chen and B. Zhao, *Nanosci. Nanotechnol. Lett.*, 2018, **10**, 1613.
27 C. Sun, X. B. Wang, X. J. Yang, L. Xing, B. Zhao, X. D. Yang and C. Mao, *Electrochim. Acta*, 2013, **106**, 327.
28 C. Sun, L. Ma, Q. H. Qian, S. Parmar, W. B. Zhao, B. Zhao and J. Shen, *Analyst*, 2014, **139**, 4216.
29 Y. G. Zhao, X. H. Chen, S. D. Pan, H. Zhu, H. Y. Shen and M. C. Jin, *Talanta*, 2013, **115**, 787.
30 J. Y. Liu, W. H. Lu, H. T. Liu, X. Q. Wu, J. H. Li and L. X. Chen, *Electrophoresis*, 2016, **37**, 2502.
31 Y. Y. Wen, J. H. Li, J. S. Liu, W. H. Lu, J. P. Ma and L. X. Chen, *Anal. Bioanal. Chem.*, 2013, **405**, 5843.
32 F. Yi, Y. L. Zheng, T. T. Wang, L. Z. Liu, Q. R. Yu, S. Y. Xu, H. L. Ma, R. Cheng, J. N. Ye and Q. C. Chu, *Chromatographia*, 2016, **79**, 619.

